



HAL
open science

Optimization of a New Reactive Force Field for Silver-Based Materials

Clement Dulong, Bruno Madebene, Susanna Monti, Johannes Richardi

► **To cite this version:**

Clement Dulong, Bruno Madebene, Susanna Monti, Johannes Richardi. Optimization of a New Reactive Force Field for Silver-Based Materials. *Journal of Chemical Theory and Computation*, 2020, 16 (11), pp.7089-7099. 10.1021/acs.jctc.0c00480 . hal-03969297

HAL Id: hal-03969297

<https://hal.science/hal-03969297>

Submitted on 2 Feb 2023

HAL is a multi-disciplinary open access archive for the deposit and dissemination of scientific research documents, whether they are published or not. The documents may come from teaching and research institutions in France or abroad, or from public or private research centers.

L'archive ouverte pluridisciplinaire **HAL**, est destinée au dépôt et à la diffusion de documents scientifiques de niveau recherche, publiés ou non, émanant des établissements d'enseignement et de recherche français ou étrangers, des laboratoires publics ou privés.

Optimization of a new reactive force field for silver-based materials

Clement Dulong¹, Bruno Madebene¹, Susanna Monti² and Johannes Richardi^{3*}

¹ Sorbonne Université, CNRS, De la Molécule aux Nano-Objets: Réactivité, Interactions Spectroscopies, MONARIS, 75005, Paris France

² CNR-ICCOM, Institute of Chemistry of Organometallic Compounds, via G. Moruzzi 1, I-56124 Pisa, Italy

³ Sorbonne Université, CNRS, Laboratoire de Chimie Théorique, LCT, 75005 Paris, France

Abstract

A new reactive force field based on the ReaxFF formalism is effectively parametrized against an extended training set of quantum chemistry data (containing more than 120 different structures) to describe accurately silver- and silver-thiolate systems. The results obtained with this novel representation demonstrate that the novel ReaxFF paradigm is a powerful methodology to reproduce more appropriately average geometric and energetic properties of metal clusters and slabs when compared to the earlier ReaxFF parametrizations dealing with silver and gold. ReaxFF cannot describe adequately specific geometrical features such as the observed shorter distances between the under-coordinated atoms at the cluster edges. Geometric and energetic properties of thiolates adsorbed on a silver Ag₂₀ pyramid are correctly represented by the new ReaxFF and compared with results for gold. The simulation of self-assembled monolayers of thiolates on a silver (111) surface does not indicate the formation of staples in contrast to the results for gold-thiolate systems.

1. Introduction

Self-assembled monolayers (SAMs) of organic molecules on metallic surfaces can be used for creating nanoimprints, biosensors, protective layers, biomimetic covers, and stabilizers to favor specific morphologies. They also serve to manipulate topological, chemical and functional features and to design complex structures that are important in a wide variety of applications. Among SAMs, thiolate layers on gold and silver surfaces have received major attention.^{1,2} In particular, these SAMs can stabilize effectively the metal nanoparticles and improve their properties when functionalized with hydrophilic or hydrophobic moieties.³ Recent investigations on SAMs adsorbed on gold surfaces have revealed the formation of S-Au-S staple motifs, which were already predicted by the theoretical methodologies.^{4,5}

The computational characterization of SAMs by quantum chemical methods such as DFT⁶⁻⁸ is usually limited to nanoparticles where the size is lower than 3 nm or small periodic slabs, but becomes impractical and too demanding when both slab and nanoparticle dimensions increase to 5 nm and beyond. In this case, two different approaches are usually employed: simulations based on force fields⁹⁻¹³ and tight-binding DFT calculations.¹⁴⁻¹⁶ **However, due to the special features of SAMs, to the metals and their mutual interactions, *ad hoc* force field parameters and formulations have been developed to obtain realistic representations.** Bond-order reactive force fields are the most appropriate solution and can be designed for describing and predicting the correct adsorption locations of the SAMs, the formation of staples, surface reconstructions and other effects¹⁷⁻²¹ important for the properties of these functionalized interfaces.

Regarding the gold/thiolate system¹⁹⁻²¹, three reactive force fields have been proposed in the past and used for various types of simulations, including bio-conjugate materials for biomedical applications.²² The excellent results, in line with the experiments, allowed to disclose different aspects of thiolate and staple formation. The success of this type of description for many other metals, such as copper,²³ silver²⁴ and cobalt²⁵ is apparent from the literature, as well. To the best of our knowledge, no ReaxFF force field has been developed yet to characterize comprehensively silver-thiolate materials and, more specifically, silver/thiolates nanocrystals. This would open up new atomistic simulations of realistic silver nanoparticles in various types of environmental conditions close to the experimental setup and will allow to better understand their properties and all the mechanisms connected to their

diffusion, reactivity and response to external stimuli. Furthermore, it will lead at long term to a possible improvement and tuning of their characteristics important for many applications. Silver nanoparticles are indeed widely used for their antimicrobial and plasmonic properties.^{26,27}

Gold and silver have many similar properties. Due to relativistic effects, the distance between the atoms in bulk gold and silver with fcc structure is close (2.87 Å).²⁸ Moreover, the adsorption of thiolates on these metals follows similar mechanisms occupying, preferentially, the bridge sites on flat (111) surfaces in DFT calculations.⁸ However, it is still an open question if the reorganization usually observed for gold⁵ also occurs for silver. Moreover, for gold and silver, essential differences appear. For example, gold is more deformable than silver, and thus gold clusters show a broader range of atomic nearest-neighbors distances compared to silver.²⁹ Moreover, SAM thiolates on silver do not adopt the classical hexagonal superstructure observed on gold.¹

The reproduction of all these features is a challenge that cannot be solved if only classical non-reactive force fields are considered. This is why we have decided to develop a new reactive force field for silver/thiolate systems and to compare the simulations results with published data to validate the improvements of our description.

The initial ReaxFF parameters of silver were extracted from the literature.²⁴ A preliminary check of the old parameters revealed that the silver clusters obtained at the DFT level could not be reproduced by the published force field (see Figure 1). Thus, all the parameters were reoptimized against a database of DFT data consisting of published structures and new optimized systems. Beside the metal, we optimized the parameters of Ag-S using new DFT data. The results for silver and silver-thiolate systems are compared with those obtained for the published gold reactive force fields. Finally, the results of the molecular dynamics simulations of SAMs on gold and silver are presented.

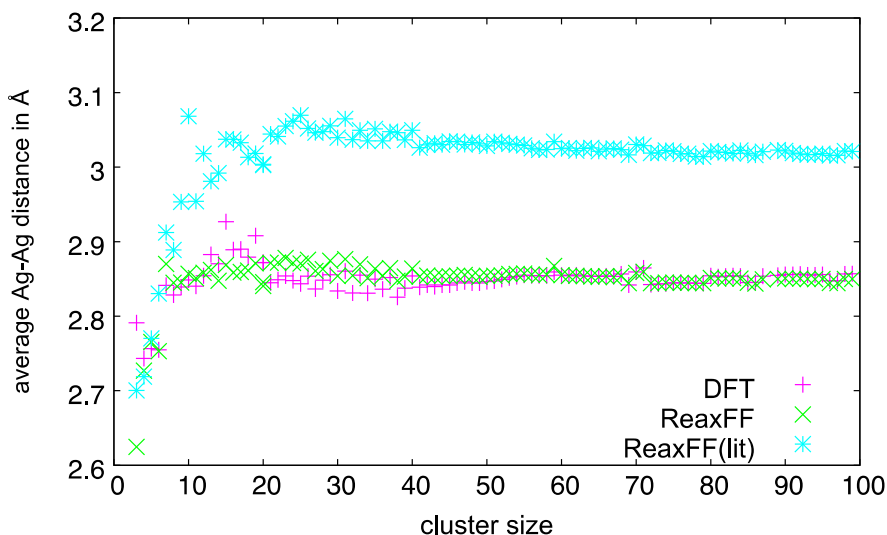


Figure 1: Average first-neighbor distances between silver atoms as a function of the cluster size (from 2 to 99 silver atoms) for DFT, the published reactive force field (ReaxFF (lit)),²⁴ and the one developed here (ReaxFF). The root mean square deviations of the ReaxFF(lit) and ReaxFF results with respect to the DFT data are 0.171 Å and 0.023 Å, respectively.

2. Methods

2.1. The ReaxFF model

In the ReaxFF approach, the energy of a system is calculated with the following equation^{30,31}:

$$E_{system} = E_{bond} + E_{angle} + E_{tors} + E_{auto} + E_{Coulomb} + E_{vdWaals} + E_{Hbond} \\ + E_{conjugation} + E_{lone-pair} + E_{over} + E_{under}$$

E_{bond} , E_{angle} and E_{tors} correspond to the two-, three- and four-body intramolecular terms, respectively. E_{auto} is the energy difference of neutral and charged atoms. $E_{Coulomb}$, $E_{vdWaals}$ and E_{Hbond} represent the electrostatic, van der Waals and hydrogen-bond interactions. The term $E_{conjugation}$ represents a possible conjugation between three or four atoms connected by alternating double bonds. $E_{lone-pair}$, E_{over} and E_{under} represent non-binding terms, a surplus and a lack of valence electrons relative to the isolated species, respectively.

This force field differs from classical force fields by the fact that all the contributions, apart from the van der Waals and electrostatic terms, are expressed as a function of the bond order.

This allows bond breaking and formation. A detailed explanation of all the terms can be found in the literature.^{30,31}

In the case of metals some of the terms are set to zero (for example, E_{angle} and E_{tors}).

Atomic charges can be calculated by the EEM method (*Electronegativity Equalization Method*) introduced by *Mortier et al.*^{32,33} or adopting the Atom-Condensed Kohn-Sham DFT approximated to second-order (ACKS2) description.³⁴ In this case, all the old parameters should be revised to guarantee compatibility with the new representation. Considering that the previous gold/silver force fields were based on the EEM method we chose this for the new development. All the simulations and force field optimizations were carried out with the ReaxFF modules integrated in the SCM/ADF³⁵ and LAMMPS^{36,37} packages.

2.2. The Parameterization of the AgSCH-ReaxFF potential with the MCFF method

The force field optimization performed in this investigation was carried out with the Monte Carlo algorithm (MCFF)³⁹ implemented in the SCM/ADF code. Even though a new method dubbed Covariance Matrix Adaptation Evolution Strategy (CMA-ES)⁴⁰ has recently been published. Its comparison with the MCFF methodology⁴¹ has revealed that both tend towards very similar results when the training set is sufficiently large, thus, the MCFF procedure was chosen to stay in line with the recent Au/S/C/H parametrization strategy reported in ref 21. A brief description is provided to give an idea of the number of possible choices that are inherent to this procedure and could bias the final results. Briefly, the generic principle of MCFF is as follows:

1) A *training set* containing experimental and theoretical data is prepared (for example, molecular geometries optimized at different levels of accuracy, their relative energies, surfaces of potential energy representing the dissociation curve between two atoms, the atomic charges of atoms, etc.). A part of the results is reserved for a validation set which shows the reliability of the parameterized force field.

2) A set of parameters is chosen and the selected parameters are optimized by minimizing the **unitless** error function:

$$Error = \sum_{i=1}^n \left[\frac{X_{i,TS} - X_{i,ReaxFF}}{\sigma_i} \right]^2$$

with n the number of points present in the training set, $X_{i,TS}$ the value of point i in the training set, $X_{i,ReaxFF}$ the corresponding value obtained by ReaxFF calculations, and σ_i the

desired precision that the point i shall take. σ_i is equal to $1/\omega_i$ with ω_i^2 the actual weight of the point in the total error.

The acceptance of the new set of parameters is determined by a probability defined as follows:

$$P_{acceptation} = \min[1, \exp(-\beta \Delta Error)]$$

with β a unitless parameter controlling the sampling in the parameter space and $\Delta Error = Error_{new} - Error_{previous}$ the difference between the new error of the system and the previous one. The initial value for β and the linear temperature increase factor are determined by the method proposed by *Shchygol et al.*⁴¹ Preliminary tests have shown that the use of eight replica is appropriate to increase the chances of getting closer to a minimum error.⁴⁰

2.3. DFT calculations

DFT calculations were carried out with the PBE functional.⁴⁴ The modLAN2DZ and 6-311++G(2d,2p) basis sets were used for Au/Ag⁴⁵ and S, C, H⁴⁶ respectively. The calculations were performed with the Gaussian09 package.⁴⁷ Gaussian and not ADF has been used here for coherence with previous investigations.

These selections were based on data found in the literature. Indeed, in 2014 *Muniz-Miranda et al.*⁴⁸ investigated systematically the behavior of more than twenty five exchange-correlation functionals (GGA, meta-GGA, Hybrid,...), including PBE, on three aggregates of Au covered with sulfur and phosphorus ligands, with different morphologies, charges, and experimental structures. This study showed that the PBE functional, coupled with the basis of Gaussian functions with pseudopotentials modLAN2DZ, leads to the results closest to the experimental data, for both structures and energy differences between the highest occupied and the lowest unoccupied molecular orbitals (HOMO-LUMO). These data suggest that PBE is appropriate for the present molecular systems.

2.4. Simulation methods

Molecular dynamics simulations in the NVE ensemble were carried out using the LAMMPS program.^{36,37} The three force fields for gold-thiolate were available in the SCM/ADF package. The force field developed for the silver-thiolate systems is included in the Supporting Information. In all the molecular dynamics simulations a time step of 0.25 fs was employed

and the temperature was controlled by the Berendsen's thermostat with a damping constant of 5 fs. The total simulation time was approximately 100 ps.

3. Results and Analysis

3.1. Force Field Optimization for silver

3.1.1. Training set and selected FF parameters

To reparameterize the potential, we used the following data:

- Several optimized clusters structures with 2 to 99 silver atoms were obtained from the supporting information of the article by Chen et al.⁵⁰ (PBE/LANL2DZ). The clusters with 2 to 20 silver atoms were re-optimized at the PBE/modLANL2DZ level of theory. All the Ag-Ag first neighbor distances ($< 3.2 \text{ \AA}$) and their Ag-Ag-Ag angles within the clusters made of 2 to 20 silver atoms were included in the training set together with the first neighbor distances in the 21-99 atom clusters (number of points in the training set: ~ 22000).
- The cluster energies per atom for Ag_2 to Ag_{99} were included in the training set. These are calculated by considering a reference. Two different references are used corresponding to the minimum energy structures for the clusters with < 20 atoms and that of the larger ones.

$$E_{cluster} = \frac{E_{Ag_n}}{n} - \frac{E_{Ag_n,ref}}{n_{ref}}$$

- The potential energy surfaces (PES) describing the dissociation of the Ag_2 dimer was included in the training set together with a second PES, which describes the dissociation of a vertex atom of an Ag_{20} pyramid. This was obtained by shifting the vertex atom of the pyramid along the central axis passing from the vertex. This was meant to reproduce the desorption of an **adatom** from a crystalline (111) surface of silver.
- The equation of state of body-centered-cubic, face-centered-cubic, and hexagonal closed packed solids was added to the training set to obtain a good description of bulk silver. These data were obtained by Lloyd et al.²⁴ who carried out DFT calculations at the PBE/DZP level (see ref 24 for more details on these computations).

The training set and its geometric files are given in the SI. The general parameters for the optimization are reported in Table 1, which shows the weights usually used in this kind of parameterization.^{21,39,41} The values of σ_i correspond to the optimization accuracy. The weights

of some data have been modified to obtain the best reproduction of the DFT values (see trainsets in SI for the actual values). To assure that the minimum of the PES is well reproduced, only those values close to the minimum were weighted $1 \text{ (kcal/mol)}^{-2}$, whereas at shorter and larger distances smaller weights were used. To reach a good reproduction of the energies for large clusters, the weight of these data has also been increased.

Type	σ_i	Weight on the total error ($1 / \sigma_i^2$)
distances	0.1 (Å)	100.0 (Å ⁻²)
angles	5°	(1/5°) ²
energies	1.0 (kcal / mol)	1.0 ((kcal / mol) ⁻²)

Table 1: Chosen accuracy in terms of σ_i and weights of the data points in the training set consisting of interatomic distances (Å), angles (in degrees) and energies (kcal/mol).

The EEM parameters of the literature have been used in the following.^{17,23} Since the charges on metallic clusters are very small, these parameters have only a slight influence on the parameterization. The FF optimization was focused on bonds, angles, and binding energies. Fifteen parameters, corresponding to atomic and interatomic terms were optimized.

3.1.2. Performance of the new silver FF in relation to the previous descriptions

Starting from the silver force field proposed in the literature,²⁴ the optimization produced a new force field with 11 % of the initial error to reproduce the data contained in the training set. The silver force field reported in the literature²⁴ will be denoted as ReaxFF (lit) in the following.

Figure 1 shows the evolution of the average first neighbor distance as a function of the cluster size for the training data (DFT structures), for the literature (ReaxFF (lit)),²⁴ and the new force fields (ReaxFF).

The evolution of the average distance of the clusters obtained with the new ReaxFF presents the same trend as the training set data. In contrast, the average distances obtained with ReaxFF(lit) are too long compared to the DFT data except for the smallest clusters. The average distance converges to 2.86 Å for large clusters (for DFT) and ReaxFF in contrast to

3.03 Å that is the value obtained for ReaxFF(lit). This improvement is also evident in the maximum deviations of the Ag-Ag distances (Figure 2).

It was noticed that the maximum deviation decreases from 0.3 Å (ReaxFF(lit)) to about 0.1 Å (new ReaxFF) for the larger clusters. The three exceptions, clearly visible in the plots (Figure 2), represent the Ag₃, Ag₁₅ and Ag₅₉ clusters. A deeper inspection of these cases and the comparison between the DFT and ReaxFF geometries revealed that they appeared for the largest bond distances predicted by DFT for surface atoms. The Ag₃ ReaxFF description predicts a perfect equilateral triangle (bond length 2.63 Å), while at the DFT level the distance between two atoms (3.06 Å) is larger than the other ones (2.65 Å). For Ag₁₅, four distances around 3.4 Å obtained by DFT were reduced by the ReaxFF to values around 2.9 Å. In the case of Ag₅₉ two atoms with a distance of 3.2 Å in DFT, were separated by ReaxFF (new distance: 3.67 Å). We anticipate that these differences may be explained by the smaller range of the attraction between silver atoms predicted by ReaxFF.

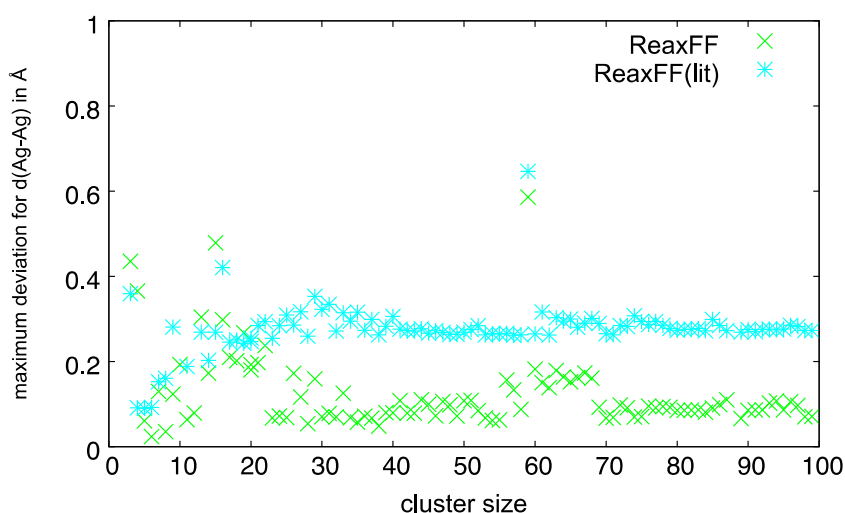


Figure 2: Maximum deviation of the first-neighbor distances for each cluster relative to the training set for the published reactive force field (ReaxFF (lit)),²⁴ and the one developed here (ReaxFF). It corresponds to the maximum absolute value of the differences between the distances obtained by ReaxFF and DFT.

In Figure 3, the DFT and ReaxFF geometries of the Ag₂₀ pyramid are compared. The structure can be completely defined by the reported distances between vertex (V), edge (E) and facet (F) atoms, which have 3, 6 and 9 first neighbors, respectively. It is apparent that the new ReaxFF does not correctly reproduce the variations of the distance within the silver pyramid, describing it as quasi-crystalline. However, also ReaxFF(lit) had problems with

atom distances and overestimated the distances between the edge and facet atoms (3.00 and 3.03 Å), which disagrees with the reference DFT data. It is evident that ReaxFF cannot describe correctly the distances between the atoms with low coordination on edges and vertices which should be usually shorter. In the case of gold (ReaxFF by *Järvi et al.* 2008¹⁷) the interatomic distances are all very close to each other (2.88 Å). Similar to Ag₂₀, the pyramid obtained with ReaxFF is a perfect crystal. It should be noted that all published force fields¹⁸⁻²¹ for gold systems are based on this model.

For all the clusters in the training set, the Ag-Ag distances obtained with the two force fields were compared to the DFT data. Figure 4 shows two typical results for a smaller (Ag₁₀) and a large cluster (Ag₉₈). The geometry of both clusters is better reproduced by the new ReaxFF. As already observed for the pyramid, the variation of distances for the small cluster obtained by the ReaxFF is more limited compared to DFT. For the larger clusters the hierarchy of distance lengths is better respected.

To study the reliability of new ReaxFF, we prepared a validation set made of all Ag-Ag-Ag angles of large clusters (~ 128000 points) which were not included in the training set. The total error obtained for this set is 30% lower than the one obtained with the published ReaxFF with a maximum angular deviation of 7°.

With regard to the reproduction of the energy data of the training set, the cluster energies and the potential dissociation energy curves of the dimer and the pyramid vertex atom are shown in Figure 5. It should be noted that the DFT curves for the dissociation of the dimer and the pyramid vertex atom were calculated taking the two possible electronic states, singlet and triplet, into account as done in *Järvi et al.*'s work on gold.¹⁷ The dissociation energy curve should be close to the minimum of the singlet DFT curve (actually here 1.2 kcal/mol for Ag₁₉-Ag) and tends to the results for the triplet at a larger distance. This is due to the fact that the triplet is more stable than the singlet at a larger distance. To obtain the agreement, we used in the training set the DFT data of the singlet curve close to the minimum and those for the triplet at larger distances. For Ag-Ag, the deviation for the dissociation energy is quite larger (5.3 kcal/mol).

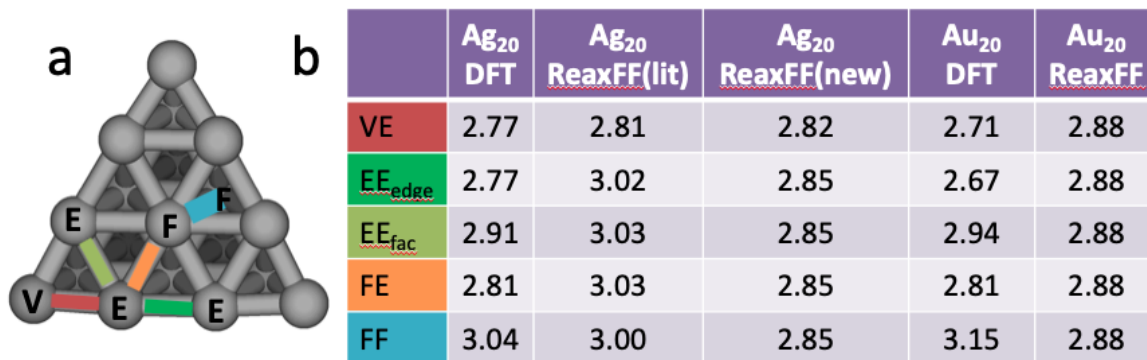
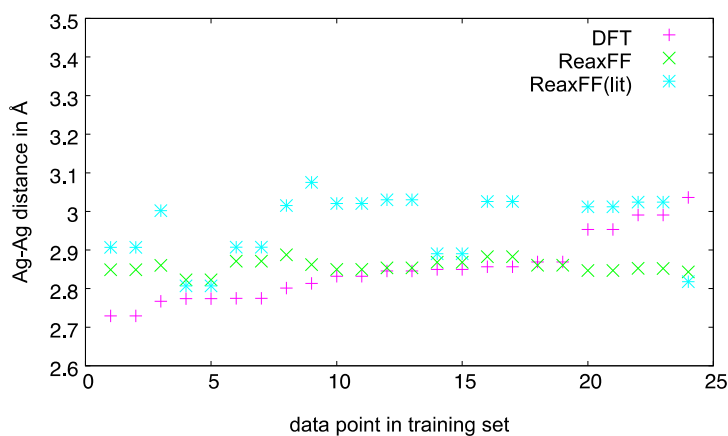


Figure 3. (a) Optimized geometry of the Ag₂₀ pyramid computed from the ReaxFF published in the literature²⁴. The vertex (V), edge (E), and facet (F) atoms are shown. (b) Comparison of DFT and ReaxFF results for silver and gold. The Ag-Ag distances are given in Å.

a



b

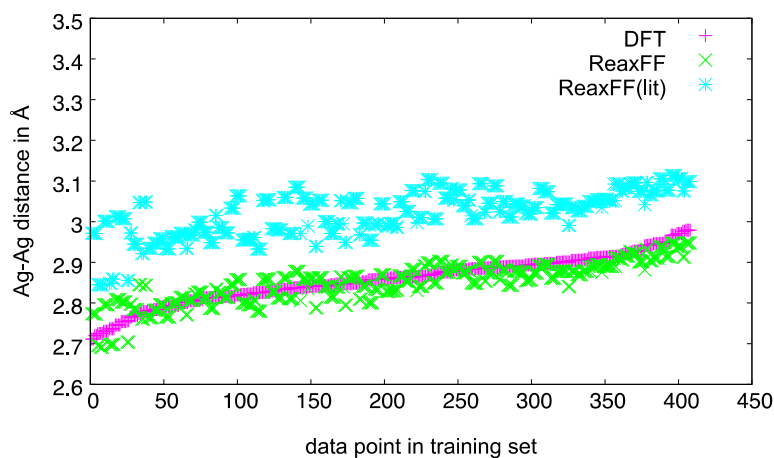
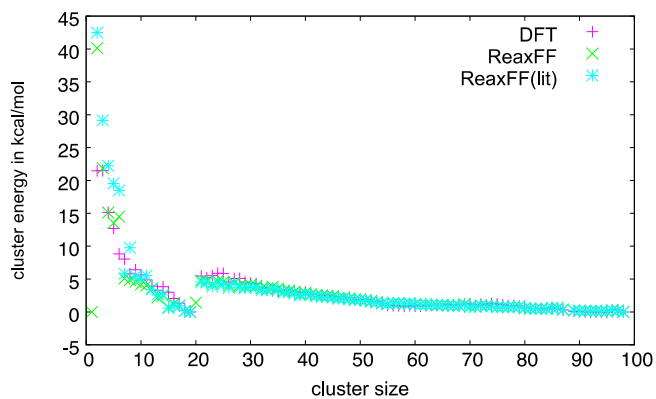


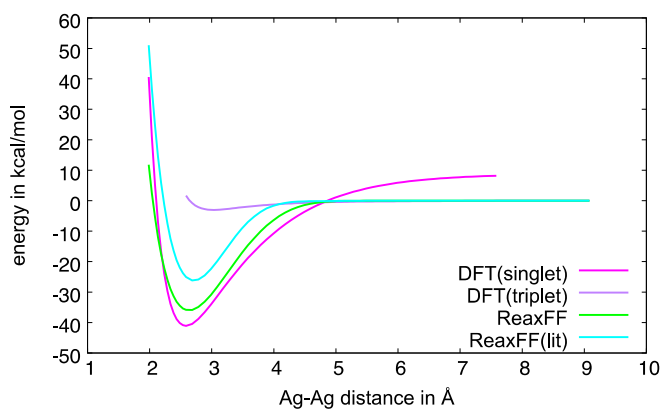
Figure 4: First-neighbor distances between silver atoms for two clusters as a function of the data point obtained by DFT, the published reactive force field (ReaxFF (lit)),²⁴

and the one developed here (ReaxFF): (a) Ag₁₀ and (b) Ag₉₈. For the Ag₁₀ (Ag₂₀) cluster the root mean square deviations of the ReaxFF(lit) and ReaxFF results with respect to the DFT data are 0.423 (0.170) and 0.085 (0.029) Å, respectively.

a



b



c

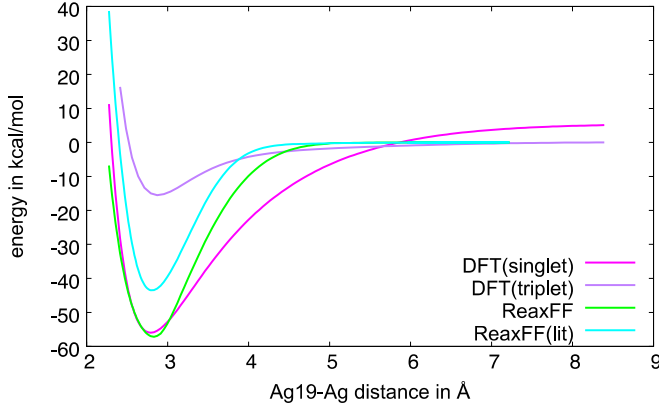


Figure 5: (a) cluster energies (in kcal / mol) for all clusters of 2 to 99 atoms, (b) potential energy surfaces of the dissociation of a silver dimer and (c) the dissociation of a vertex atom of the pyramid as a function of the distance between the vertex atom and its closest neighbor on the edge. Results obtained by DFT, the published reactive force field (ReaxFF (lit)),²⁴ and the one developed here (ReaxFF). The root mean square deviations of the ReaxFF(lit) and ReaxFF with respect to the DFT data are 0.171 Å and 0.023 Å, respectively.

The new ReaxFF respects the hierarchy of cluster energies, slightly improving the absolute values of the energies of small silver clusters of 2 to 20 atoms relative to ReaxFF(lit). The dissociation energies of the dimer and the pyramid vertex atom are significantly improved at the minimum equilibrium energy level, with an error of 1.2 kcal/mol in the case of the pyramid compared to 15 kcal/mol for the previous model. Nevertheless, due to the exponential function modeling the dissociation of the bonds in the ReaxFF ($E_{bond} = -D_e \cdot BO_{ij} \cdot \exp[p_{be,1} \cdot (1 - BO_{ij}^{p_{be,2}})]$), the range of the attraction peak is shorter compared with the DFT data. (As shown in table SII in SI, both parameters $p_{be,1}$ and $p_{be,2}$ have been optimized.) This could be a possible explanation of the problems observed in Figure 1 for Ag_3 , Ag_{16} and Ag_{59} as discussed above. The ReaxFF tends to connect or separate atoms that are at intermediate distances larger than 3 Å.

For the EOS energies of body-centered cubic, face-centered cubic, and hexagonal closed packed solids, the newReaxFF is quite correct. Figure 6 illustrates the case of face-centered cubic solid. The Ag-Ag equilibrium position is 2.85 Å instead of 3.01 Å according to the data of the training set given by Lloyd et al.²⁴ (which we have integrated into our set, as discussed above). It should be emphasized that the DFT calculations by Lloyd et al. do not correctly describe the Ag-Ag distance with respect to the experimental values (2.87 Å).²⁸ This explains

the disagreement between DFT and ReaxFF(lit) observed for example for the Ag-Ag distance in the clusters (see Figure 1). The new Ag-Ag equilibrium position of 2.85 Å better agrees with the experiment and confirms the validity of the new ReaxFF.

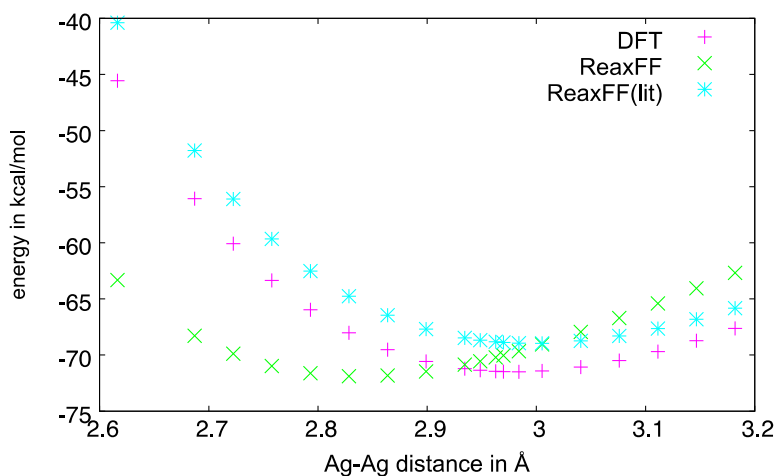


Figure 6: Energy of expansion of a cubic-face centered solid as a function of the Ag-Ag distance obtained by DFT, the published reactive force field (ReaxFF(lit)),²⁴ and the one developed here (ReaxFF). The Ag-Ag equilibrium distance experimentally observed is 2.87 Å.²⁸

3.2. Ag - S potential parameterization

3.2.1. Training data and parameters selection

To establish a training set for the adsorption of thiolate molecules on silver clusters and nanoparticles, we studied the MeS-Ag₂₀ isomers. The silver pyramid was chosen since it meets the following criteria important for the parameterization:

- Its geometry is close to a face-centered cubic structure typical of many silver clusters and crystalline nanoparticles.
- It possesses specific sites: facets, edges and vertices.
- It is large enough to behave as large clusters.
- It is sufficiently small to allow DFT calculations at a reasonable computational cost.

As illustrated in Figure 3, the pyramid has three distinguishable types of atoms: vertex atoms, edge and facet atoms. The geometry optimizations in the most stable electronic state (open-shell doublet) only led to the occupation of five adsorption sites by MeS, common to gold and silver: one on top (V) and four on bridge sites (EE_{edge}, VE, FE, EE). Here, the sites are named according to the atom types involved. For the FE and EE sites, a distinction between two isomers at the same site can be made according to the orientation of the methyl

(up or down). This leads to seven different isomers (V, EE_{edge}, VE, FE_{up}, EE_{up}, FE_{down}, EE_{down}).

The geometric data considered in the training set were the Ag-S interatomic distances of the seven MeS-Ag₂₀ isomers, and the Ag-S-Ag and Ag-Ag-S angles, which defined the correct adsorption geometry of the thiolates on the metal part. The interatomic Ag-Ag distances were also retained in the training set to include the impact of the Ag-S interaction on the deformation of the silver pyramid in the error function.

For the energetic terms, the dissociation curves of a silver atom with a thiolate, the potential energy surface of the variation of the Ag-S-Ag angle on a silver dimer, and the relative energies of our MeS-Ag₂₀ isomers were included. These choices were motivated by the study of the training set used by *Järvi et al.*^{17,19}

EEM parameters were not optimized.^{17,21} From our quantum calculations it was found that the Mulliken charges for the isomers were not appropriate. Indeed, for the isomer EE_{edge}, for example, sulfur was positively charged (+0.6) and the metal atoms interacting with S negatively charged (-0.3), which is the opposite in the case of the *Bader* and NPA descriptions. Therefore, we decided to avoid the optimization of EEM parameters with Mulliken charges.

In total, the training set contained 1566 points. The weights were increased to focus the optimization on distances and angles. For the Ag-S distances and the Ag-S-Ag and Ag-Ag-S angles, an accuracy of 0.01 Å and 1°, respectively, was selected. On the contrary, the accuracy of the Ag-Ag and Ag-Ag-Ag angles within the pyramids were kept at 0.1 Å and 5.0° except for the bonds between two Ag atoms in direct contact with S (0.01 Å).

The initial set of parameters was extracted from the literature.²¹ The Au-H and Au-C parameters obtained by Monti et al. were used for the Ag-H and Ag-C interaction. The training set considered in this work cannot be employed for optimizing these parameters. Only the interatomic parameters acting on the Ag-S bonds (distance and strength), without pi and pi-pi bonds, and the parameters describing the two types of Ag-S-Ag and Ag-Ag-S angles were improved. In total, 23 parameters were optimized.

3.2.2. Results and comparison for the Ag-S force fields

The best force field obtained corresponded to a reduction of the error around 15 % (with respect to the parameters of Au-S). Figure 7 illustrates the geometric comparisons of the MeS-Ag₂₀ isomers and their relative energies between the ReaxFF and DFT data. Only the

down isomers are shown for FE and EE, since the results for the up counterparts are very similar. The histograms from left to right represent the Ag-S distances and all the Ag-Ag interatomic distances of the silver atoms in contact with sulfur. The following results were obtained:

- The energy hierarchy is very well reproduced by ReaxFF, with $EE_{\text{edge}} < VE < FE_{\text{down}} \approx V \approx EE_{\text{down}}$.
- According to the histograms of the interatomic distances, the Ag-S distances are well reproduced for all isomers (difference less than 0.1 Å).
- In the case of the bridged isomers, the elongations of the distance between the both Ag atoms in contact with sulfur are in good agreement with the DFT results.
- The global reorganization of the pyramid suffers from the tendency to favor crystalline descriptions. Thus, ReaxFF does not reproduce the extraction of facet atoms, predicting FF distances similar to the other Ag-Ag distances, see the two distances FF for the FE_{down} isomer. For the same isomer, an elongation of the EE_{edge} distance is predicted by ReaxFF which is not observed by DFT.

Relative energies (kcal/mol)

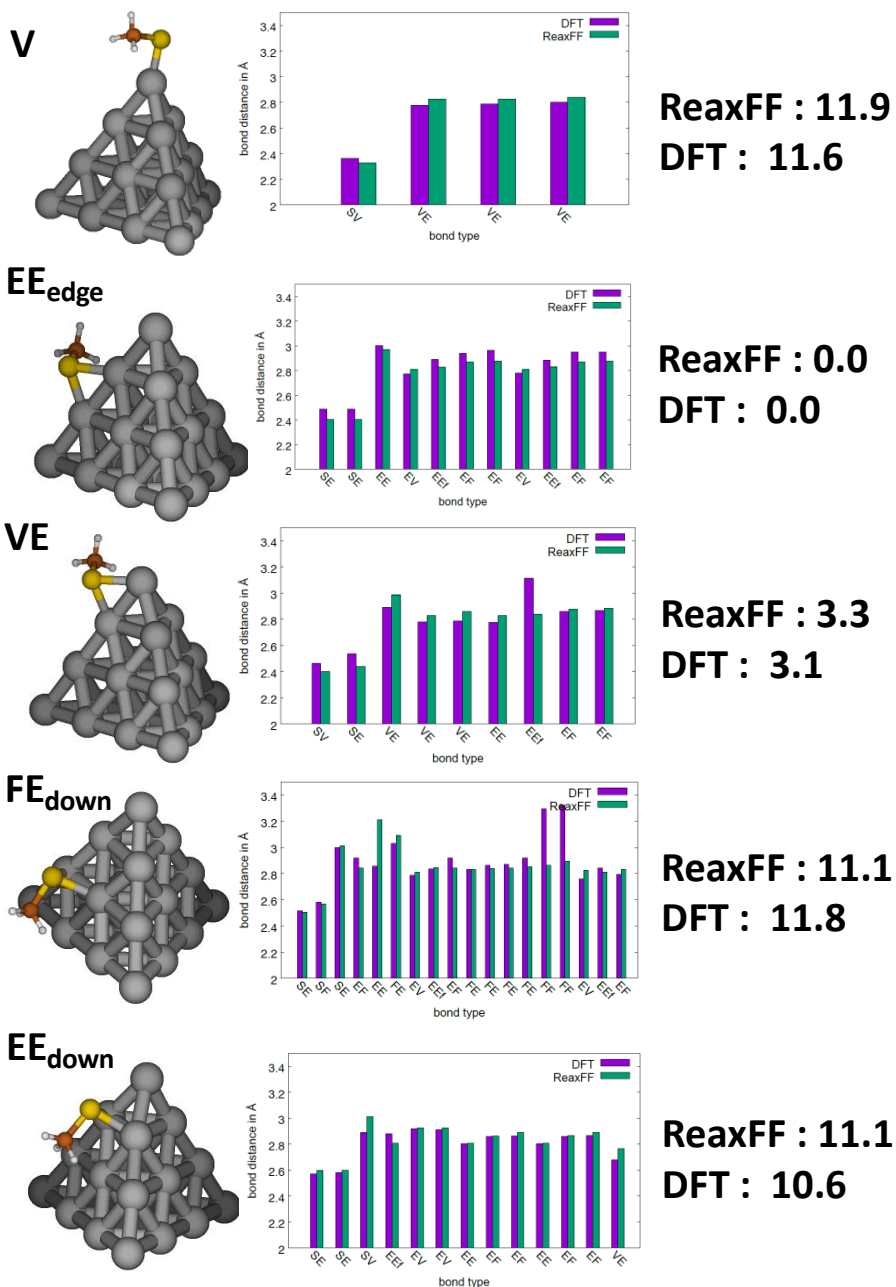


Figure 7: Optimized geometries, relevant interatomic distances and relative energies (kcal / mol) obtained by ReaxFF and DFT for each MeS-Ag₂₀ isomers.

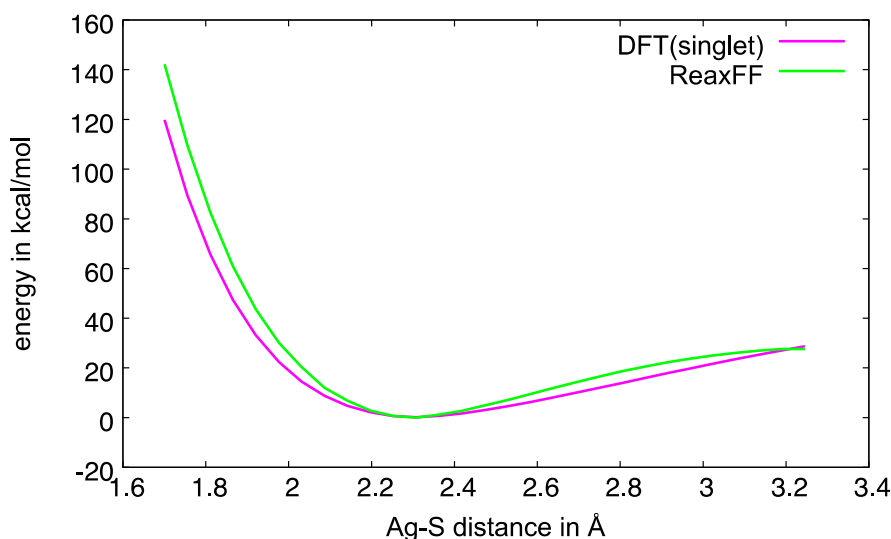


Figure 8: Potential energy surface of the dissociation of MeS-Ag (kcal / mol).

The potential energy curve of MeS-Ag dissociation obtained with the new force field and DFT are shown in Figure 8. In the case of AgS the singlet is more stable than the triplet and the results can be directly compared with this curve. The dissociation curve is well reproduced. The equilibrium of the Ag-S-Ag angle is around 71° , which corresponds to the angles found for the MeS-Ag₂₀ isomers by DFT.

To see if ReaxFF was capable of reproducing the differences between the adsorption on gold and silver as observed by DFT, we carried out the same comparison made in the case of the MeS-Au₂₀ isomers. All isomers obtained by DFT calculations were optimized with the three ReaxFF published¹⁹⁻²¹ and the structural and energy data were collected in table S1 in the SI. The three ReaxFF are denoted by the first author of the corresponding articles: Järvi, Bae and Monti.¹⁹⁻²¹ Please note that for the ReaxFF of Bae and Aikins, the parameters published in table SII of this article²⁰ (denoted by NP specific) have been used. These parameters were chosen, since in this article it has been stated that they should better work for nanoparticles. Figure S1 shows the final structures obtained by the different methods. Usually, ReaxFF does not reproduce exactly the geometry obtained with DFT, while for silver a good agreement was found. This is not surprising since the models were not optimized using thiolates adsorbed on clusters but on metallic surfaces. To clarify we will discuss the EE_{edge} isomer as an example. In the case of gold, the Au-S distance of this isomer should be 0.12 Å shorter than for silver, while the bond between the Au atoms in contact with S should be 0.25

Å larger. These differences are not reproduced by ReaxFF, which obtains a similar distance for both metals. It is interesting to note that the three ReaxFF can predict qualitatively different structures. Thus, for the V isomer in the case of the Monti potential, the Au-S interaction is identical to that of our DFT reference. The Au-S bond is vertical and parallel to the central rotation axis of the pyramid. In the case of the other two potentials, the Au-S distance is too large, and the axis of the Au-S bond is almost parallel to an edge ($\text{S-Au(V)-Au(E)} = 167^\circ$). Two different geometries also appear during the optimization of the EE_{down} isomer: the first one, obtained from the Bae potential, does not have a metal-ligand interaction, the ligand being separated from the pyramid. In the case of the *Järvi* and *Monti* potentials, the geometry obtained has an interaction site that is closer to a *hollow* site than to the bridged site obtained in DFT.

With respect to the energy data, the hierarchy of isomers calculated with *Järvi* potential is closest to the DFT hierarchy. That of *Bae* clearly shows a very bad reproduction of energies, in particular, the V isomer is the most stable one. *Monti*'s potential seems to favor the bridge sites on the edges of the clusters. The energetic difference between ReaxFF and DFT are usually larger than those observed between silver and gold.

3.3. Application of the Ag-thiolate ReaxFF to self-assembled monolayers

To validate and test the performance of the new force field, molecular dynamics simulations were carried out to characterize the adsorption of thiolates assembled on the (111) facets of silver and gold slabs. The initial structures corresponded to one published by Groenbeck et al.⁴⁹ which is a hexagonal assembly of four thiolates on the Au(111) surface. The size of this model was increased by replication (duplication in all directions) giving a final number of 36 thiolates. For comparison, the same configuration was employed for simulating the adsorption on silver, even though from experiments it was clear that other SAM arrangements could be more stable than the selected case. The aim of these calculations was just to see if the new ReaxFF was capable of predicting different structures starting from a similar SAM arrangement on two different metals. The simulations were carried out for methane and hexane thiolates. In the case of gold the three published force fields were used, while for silver only *the* new ReaxFF was employed.

The initial structures were first minimized and then equilibrated at $T=300\text{K}$, slowly increasing the temperature (Berendsen thermostat), in the NVT ensemble.

Figure 9 shows three snapshots at 100 K in the case of gold (*Järvi* and *Monti* FFs – Figure9(a,b)) and silver surfaces (Figure 9c) in the case of hexanethiolates. In the lower right

edge, the SAM is shown without the hexane above. All snapshots for methane and hexane thiolate at 100 and 300 K are shown in the Supporting Information. In the case of the NP-specific ReaxFF proposed by Bae and Atkins²⁰, the thiolates desorbed when the temperature was increased, leading to the formation of S-S bonds (see Figure S9 in SI). To check the validity of these simulations, they were carried out with LAMMPS and ADF using a slow increase of temperature and they both resulted in a similar desorption phenomenon. This suggests that this specific force field cannot be used for simulating thiolates on gold surfaces. It should be noted that Bae and Aikins²⁰ had already written that this force field should not be used for this kind of systems. We also verified if the same problem exists for the force field of table 1 in the article by Bae and Aikins²⁰. In the final SAM configuration, obtained by hundreds of picosecond NVE simulations, the thiolates were stably adsorbed on the surface, which shows that desorption only occurs with the NP-specific model (see figure 9 in SI). The snapshots obtained for gold-thiolates is markedly different from the Järvi and Monti ReaxFF representations. In the first case (and also for the force field by Bae published in table 1 of their article), a well-ordered SAM is observed, but the gold atoms remain within the surface layer. On the contrary, the Monti potential allows reconstructions, some sulfur atoms leave the top layer and form chains of Au-S-Au staples. This is in agreement with experimental results indicating the formation of staples.^{2,5} Another, reproduced feature was that the structure of SAMs did not change when the temperature was increased to 300 K. In the case of silver, a hexagonal SAM was observed but no indication of the formation of staples was apparent. Increasing the temperature from 100 to 300 K the assembly became more irregular (see figures in the Supporting Information).

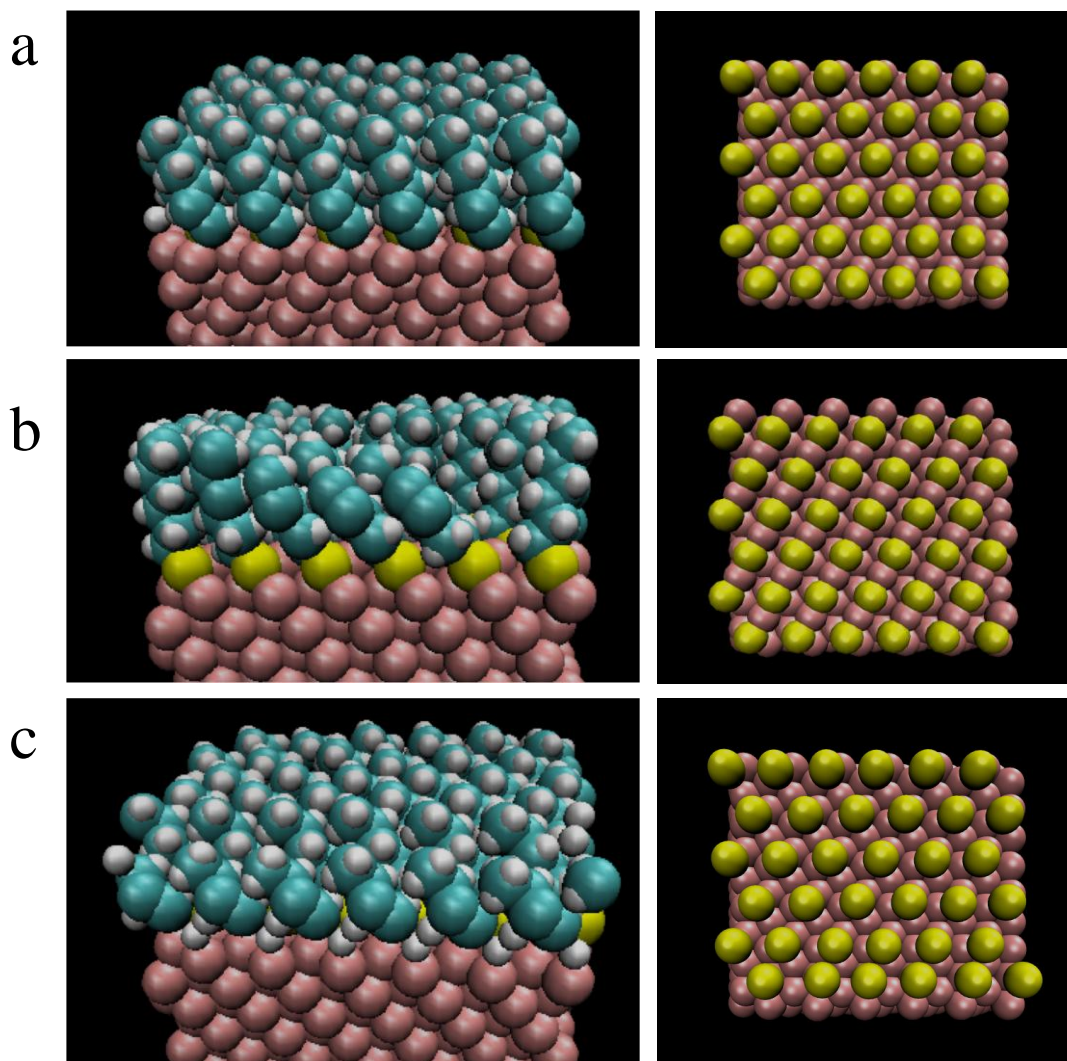


Figure 9. Snapshots of simulations of a SAM of hexanethiolate on (a) gold (ReaxFF proposed by Järvi et al.), (b) gold (ReaxFF proposed by Monti et al.), (c) silver (new ReaxFF), at 100 K. On the lower right edge, the alkane chains have been removed to see the assembly of sulfur atoms.

4. Conclusions

In this long and laborious investigation, a new reactive force field, tuned to simulate silver- and silver-thiolate-based materials, is developed. The Ag-Ag potential has been improved with respect to the one published in the literature. using a large training set consisting of DFT data of clusters of different sizes. Several hundred tests were performed, to identify the atomic and interatomic parameters essential for the reproduction of the data. ReaxFF is capable of predicting correctly the evolution of the average distance between the silver atoms of all the clusters and average energetic properties even though it fails to reproduce the smaller

distances of under-coordinated atoms located on the edges of clusters. We could speculate that only with the inclusion of other terms in the equations these tendencies could be re-modulated.

Our new Ag-S potential is very efficient for exploring the adsorption of the SAMs, characterizing the dynamics of the thiolate-silver systems and reproducing realistic structural and energetic properties of the isomers. Regarding the published ReaxFF for Au-S interactions, each potential correctly reproduces specific characteristics of the isomers: the *Järvi* potential gives a suitable energy hierarchy, the potential by *Bae* best reproduces the Au-S-Au angles, and the potential Monti provides the best description of the Au-S distances.

To enable an easy use of the new force field, we added the text file of the force field and the directory of the simulation of a SAM of hexanethiolates on Ag(111) (corresponding to figure 9c) with the input and output files for lammps simulations. Even though the developed force field is not perfect the results of the simulations are promising, in agreement with quantum chemistry calculations and experimental data. In future, it will be interesting to integrate other structures such as the $\text{Ag}_{44}(\text{SR})_{30}$ and $\text{Ag}_{25}(\text{SR})_{18}$ clusters or surfaces into the training sets to improve the proposed force field.

Acknowledgements. We thank Prof. van Duin for a fruitful exchange. This work was granted access to the HPC resources of CINES/IDRIS/TGCC under the allocation 2020-A0080811426 (Responsible: J. Richardi) made by GENCI.

* Address correspondence to Johannes.Richardi@sorbonne-universite.fr

References

1. Woodruff, D. P. The interface structure of n-alkylthiolate self-assembled monolayers on coinage metal surfaces. *Phys. Chem. Chem. Phys.* **2008**, 10, 7211-7221.
2. Häkkinen H. The gold-sulfur interface at the nanoscale. *Nat. Chem.* **2012**, 4, 443-455.
3. Daniel, M. C.; Astruc, D. Gold nanoparticles: assembly, supramolecular chemistry, quantum-size-related properties, and applications toward biology, catalysis, and nanotechnology. *Chem. Rev.* **2005**, 104, 293-346.
4. Jadzinsky, P. D.; Calero, G.; Ackerson, C. J.; Bushnell, D. A.; Kornberg, R. D. Structure of a thiol monolayer-protected gold nanoparticle at 1.1 Å resolution. *Science* **2007**, 318, 430-433.
5. Cossaro, A.; Mazzarello, R.; Rousseau, R.; Casalis, L.; Verdini, A.; Kohlmeyer, A.; ... Scoles, G. X-ray diffraction and computation yield the structure of alkanethiols on gold (111). *Science* **2008**, 321, 943-946.

6. Torres, E.; Blumenau, A. T.; Biedermann, P. U. Mechanism for phase transitions and vacancy island formation in alkylthiol/Au (111) self-assembled monolayers based on adatom and vacancy-induced reconstructions. *Physical Review B* **2009**, 79(7), 075440.
7. Grönbeck, H.; Häkkinen, H.; Whetten, R. L. Gold-thiolate complexes form a unique $c(4 \times 2)$ structure on Au(111). *J. Phys. Chem. C* **2008**, 112, 15940–15942.
8. Li, A.; Piquemal, J. P.; Richardi, J.; Calatayud, M. Butanethiol adsorption and dissociation on Ag (111): A periodic DFT study. *Surf. Sci.* **2016**, 646, 247-252.
9. Luedtke, W. D.; Landman, U. Structure and thermodynamics of self-assembled monolayers on gold nanocrystallites. *J. Phys. Chem. B* **1998**, 102, 6566-6572.
10. Rapino, S.; Zerbetto, F. Dynamics of thiolate chains on a gold nanoparticles. *Small* **2007**, 3, 386-388.
11. Pool, R.; Schapotschnikow, P.; Vlugt, T. J. Solvent effects in the adsorption of alkyl thiols on gold structures: A molecular simulation study. *J. Phys. Chem. C* **2007**, 111, 10201-10212.
12. Lane, J. M. D.; Grest, G. S. (2010). Spontaneous asymmetry of coated spherical nanoparticles in solution and at liquid-vapor interfaces *Phys. Rev. Lett.* **2010**, 104, 235501.
13. Djebaili, T.; Richardi, J.; Abel, S.; Marchi, M. Atomistic simulations of the surface coverage of large gold nanocrystals *J. Phys. Chem. C* **2013**, 117, 17791-17800.
14. Mäkinen, V.; Koskinen, P.; Häkkinen, H. Modeling thiolate-protected gold clusters with density-functional tight-binding. *Eur. Phys. J. D* **201**, 67, 38.
15. Fihey, A.; Hettich, C.; Touzeau, J.; Maurel, F.; Perrier, A.; Köhler, C.; ... Frauenheim, T. SCC- DFTB parameters for simulating hybrid gold- thiolates compounds. *J. Comp. Chem.* **2015**, 36, 2075-2087.
16. Tarrat, N.; Rapacioli, M.; Cuny, J.; Morillo, J.; Heully, J. L.; Spiegelman, F. Global optimization of neutral and charged 20-and 55-atom silver and gold clusters at the DFTB level. *Comp. Theor. Chem.* **2017**, 1107, 102-114.
17. Järvi, T. T.; Kuronen, A.; Hakala, M.; Nordlund, K.; Van Duin, A. C. T.; Goddard, W. A.; Jacob, T. Development of a ReaxFF description for gold. *Eur. Phys. J. B* **2008**, 66, 75-79.
18. Keith, J. A.; Fantauzzi, D.; Jacob, T.; Van Duin, A. C. Reactive forcefield for simulating gold surfaces and nanoparticles. *Physical Review B* **2010**, 81, 235404.
19. Järvi, T. T.; Van Duin, A. C.; Nordlund, K.; Goddard III, W. A. Development of interatomic reaxff potentials for Au–S–C–H systems. *J. Phys. Chem. A* **2011**, 115, 10315-10322.
20. Bae, G. T.; Aikens, C. M. Improved ReaxFF Force Field Parameters for Au–S–C–H Systems. *J. Phys. Chem. A* **2013**, 117, 10438-10446.
21. Monti, S.; Carravetta, V.; Ågren, H. Simulation of gold functionalization with cysteine by reactive molecular dynamics. *J. Phys. Chem. Lett.* **2016**, 7, 272-276.

22. Monti, S.; Barcaro, G.; Sementa, L.; Carravetta, V.; Ågren, H. Dynamics and self-assembly of bio-functionalized gold nanoparticles in solution: Reactive molecular dynamics simulations *Nano Res.* **2018**, 11, 1757-1767.
23. Yeon, J.; Adams, H. L.; Junkermeier, C. E.; van Duin, A. C.; Tysoe, W. T.; Martini, A. Development of a ReaxFF force field for Cu/S/C/H and reactive MD simulations of methyl thiolate decomposition on Cu (100). *J. Phys. Chem.B* **2017**, 122, 888-896.
24. Lloyd, A.; Cornil, D.; Van Duin, A. C. T.; van Duin, D.; Smith, R.; Kenny, S. D.; ... Beljonne, D. Development of a ReaxFF potential for Ag/Zn/O and application to Ag deposition on ZnO *Surf. Sci.* **2016**, 645, 67-73.
25. Zhang, X.-Q.; Iype, E.; Nedeia, S. V.; Jansen, A. P. J.; Szyja, B. M.; Hensen, E. J. M.; van Santen, R. A. Site Stability on Cobalt Nanoparticles: A Molecular Dynamics ReaxFF Reactive Force Field Study, *J. Phys. Chem. C* **2014**, 118, 6882-6886
26. Morones, J. R.; Elechiguerra, J. L.; Camacho, A.; Holt, K.; Kouri, J. B.; Ramirez, J. T.; Yacaman, M.J. The bactericidal effect of silver Nanoparticles, *Nanotechnology* **2005**, 16, 2346–2353
27. Jain, P. K.; Huang, X.; El-Sayed, I. H.; El-Sayed, M. A. Noble Metals on the Nanoscale: Optical and Photothermal Properties and Some Applications in Imaging, Sensing, Biology, and Medicine, *Acc. Chem. Res.* **2008**, 41, 1578-1586
28. Weast, R. C.; Astle, M. J.; Beyer, W. H. *CRC handbook of chemistry and physics* (Vol. 69). 1988, Boca Raton, FL: CRC press.
29. Greenwood, N. N.; Earnshaw, A. *Chemistry of the Elements*, 2nd edition, 1997.
30. Van Duin, A. C.; Dasgupta, S.; Lorant, F.; Goddard, W. A. ReaxFF: a reactive force field for hydrocarbons *J. Phys. Chem.A* **2001**, 105, 9396-9409.
31. Chenoweth, K.; Van Duin, A. C.; Goddard, W. A. ReaxFF reactive force field for molecular dynamics simulations of hydrocarbon oxidation *J. Phys. Chem. A* **2008**, 112, 1040-1053.
32. Mortier, W. J.; Ghosh, S. K.; Shankar, S. Electronegativity-equalization method for the calculation of atomic charges in molecules *J. Am. Chem. Soc.* **1986**, 108, 4315-4320.
33. Janssens, G. O.; Baekelandt, B. G.; Toufar, H.; Mortier, W. J.; Schoonheydt, R. A. Comparison of cluster and infinite crystal calculations on zeolites with the electronegativity equalization method (EEM). *J. Phys. Chem.* **1995**, 99, 3251-3258.
34. Verstraelen, T.; Ayers, P. W.; Van Speybroeck, V.; Waroquier, M. ACKS2: Atom-condensed Kohn-Sham DFT approximated to second order. *J. Chem. Phys.* **2013**, 138, 074108.
35. ReaxFF 2019.3, SCM, Theoretical Chemistry, Vrije Universiteit, Amsterdam, The Netherlands, <http://www.scm.com>, contributors: A.C.T. van Duin, W.A. Goddard, M.M. Islam, H. van Schoot, T. Trnka, A.L. Yakovlev
36. Plimpton S., Fast Parallel Algorithms for Short-Range Molecular Dynamics. *J. Comp. Phys.* **1995**, 117, 1-19.

37. Aktulga, H. M.; Fogarty, J. C.; Pandit, S. A.; Grama, A. Y. Parallel reactive molecular dynamics: Numerical methods and algorithmic techniques. *Parallel Computing* **2012**, 38, 245-259.
38. van Duin, A. C.; Baas, J. M.; Van De Graaf, B. Delft molecular mechanics: a new approach to hydrocarbon force fields. Inclusion of a geometry-dependent charge calculation; *J. Chem. Soc., Faraday Transactions* **1994**, 90, 2881-2895.
39. Iype, E.; Hütter, M.; Jansen, A. P. J.; Nedeia, S. V.; Rindt, C. C. M. Parameterization of a reactive force field using a Monte Carlo algorithm. *J. Comp. Chem.* **2013**, 34, 1143-1154.
40. Trnka, T.; Tvaroska, I.; Koca, J. Automated Training of ReaxFF Reactive Force Fields for Energetics of Enzymatic Reactions, *J. Chem. Theory and Comp.* **2017**, 14, 291-302.
41. Shchygol, G.; Yakovlev, A.; Trnka, T.; CT van Duin, A.; Verstraelen, T.. ReaxFF Parameter Optimization with Monte-Carlo and Evolutionary Algorithms: Guidelines and Insights **2019**, *J. Chem. Theory Comput.* 15, 12, 6799–6812.
42. Metropolis, N.; Rosenbluth, A. W.; Rosenbluth, M. N.; Teller, A. H.; Teller, E. Equation of state calculations by fast computing machines *J. Chem. Phys.* **1953**, 21, 1087-1092.
43. Kirkpatrick, S.; Gelatt, C. D.; Vecchi, M. P. Optimization by simulated annealing. *Science*, **1983**, 220, 671-680.
44. Perdew, J. P.; Burke, K.; Ernzerhof, M. Generalized gradient approximation made simple. *Phys. Rev. Lett.* **1993**, 77, 3865.
45. Couty, M.; Hall, M. B. Basis sets for transition metals: Optimized outer p functions. *J. Comp. Chem.* **1996**, 17, 1359-1370.
46. Frisch, M. J.; Pople, J. A.; Binkley, J. S. Self-consistent molecular orbital methods 25. Supplementary functions for Gaussian basis sets, *J. Chem. Phys.* **1984**, 80, 3265-3269.
47. Gaussian 09, Revision A.02, M. J. Frisch, G. W. Trucks, H. B. Schlegel, G. E. Scuseria, M. A. Robb, J. R. Cheeseman, G. Scalmani, V. Barone, G. A. Petersson, H. Nakatsuji, X. Li, M. Caricato, A. Marenich, J. Bloino, B. G. Janesko, R. Gomperts, B. Mennucci, H. P. Hratchian, J. V. Ortiz, A. F. Izmaylov, J. L. Sonnenberg, D. Williams-Young, F. Ding, F. Lipparini, F. Egidi, J. Goings, B. Peng, A. Petrone, T. Henderson, D. Ranasinghe, V. G. Zakrzewski, J. Gao, N. Rega, G. Zheng, W. Liang, M. Hada, M. Ehara, K. Toyota, R. Fukuda, J. Hasegawa, M. Ishida, T. Nakajima, Y. Honda, O. Kitao, H. Nakai, T. Vreven, K. Throssell, J. A. Montgomery, Jr.; J. E. Peralta, F. Ogliaro, M. Bearpark, J. J. Heyd, E. Brothers, K. N. Kudin, V. N. Staroverov, T. Keith, R. Kobayashi, J. Normand, K. Raghavachari, A. Rendell, J. C. Burant, S. S. Iyengar, J. Tomasi, M. Cossi, J. M. Millam, M. Klene, C. Adamo, R. Cammi, J. W. Ochterski, R. L. Martin, K. Morokuma, O. Farkas, J. B. Foresman, and D. J. Fox, Gaussian, Inc.; Wallingford CT, 2016.

48. Muniz-Miranda, F.; Menziani, M. C.; Pedone, A. Assessment of Exchange-Correlation Functionals in Reproducing the Structure and Optical Gap of Organic-Protected Gold Nanoclusters *J. Phys. Chem. C* **2014**, *118*, 7532.
49. Grönbeck, H.; Häkkinen, H.; Whetten, R.L. Gold-Thiolate Complexes Form a Unique $c(4 \times 2)$ Structure on Au(111). *J. Phys. Chem. C* **2008**, *112*, 15940–15942.
50. Chen, M.; Dyer, J. E.; Li, K.; Dixon, D. A. Prediction of structures and atomization energies of small silver clusters, $(Ag)_n$, $n < 100$. *J. Phys. Chem. A* **2013**, *117*, 8298-8313.
51. Kroon-Batenburg, L. M. J.; Van Duijneveldt, F. B. The use of a moment-optimized DZP basis set for describing the interaction in the water dimer. *Journal of Molecular Structure: THEOCHEM* **1985**, *121*, 185-199.